Structural model of amorphous silicon annealed with tight binding

N. Bernstein,[1] J. L. Feldman,[1,2] and M. Fornari[3]
[1]*Center for Computational Material Science, Naval Research Laboratory, Washington DC 20375, USA*
[2]*School of Computational Science, George Mason University, Fairfax, Virginia, 22030, USA*
[3]*Department of Physics, Central Michigan University, Mt. Pleasant, Michigan, 48859, USA*
(Received 15 January 2006; revised manuscript received 18 September 2006; published 8 November 2006)

We present a model of amorphous silicon generated by extensive annealing of a continuous random network structure using a molecular dynamics simulation with forces computed by a tight-binding total energy method. We also produce a refined model by relaxing the annealed model using density functional theory. Our annealed structure is primarily a fourfold coordinated continuous random network, with a few coordination defects. The first peak of the pair correlation function of the annealed structure is sharper and more symmetric than the unannealed structure, a result confirmed in the density-function-theory relaxed structure and in good agreement with static disorder results from recent x-ray diffraction analysis by Laaziri *et al.* The density, bond angle distribution function, elastic constants, and vibrational density of states of the initial and annealed structures are similar. The energy of the annealed structure is lower for both tight-binding and density-functional theory, indicating that the structure with coordination defects is energetically favored. The electronic structure of the annealed structure, computed with both charge-self-consistent tight-binding and density-functional theory, has a wide gap with several occupied gap states.

DOI: 10.1103/PhysRevB.74.205202 PACS number(s): 61.43.Dq, 61.72.Ji, 71.15.Nc, 71.15.Mb

I. INTRODUCTION

Amorphous silicon (*a*-Si) is a model system for amorphous covalent materials, and it is closely related to hydrogenated *a*-Si, which is technologically important as an inexpensive semiconducting material for electronics and photovoltaic applications. It is believed to be primarily or entirely tetrahedrally coordinated, but with no long range order.[1] The assumption behind most theoretical work is that the continuous random network (CRN) model, where every atom has four-fold coordination, is the lowest energy structure for *a*-Si.[2] There is, however, no strong justification for this assumption beyond chemical intuition. Simulations that attempt a realistic description of the energetics of bonding typically show some coordination defects, in particular five-fold coordination. This observation is often attributed to the influence of initial conditions, usually liquid silicon, and limited time scale for annealing.[3] Experiments, on the other hand, usually show coordination close to but less than than 4, but the accuracy of these results are dependent on experimental limitations and assumptions that influence the data analysis.

Here we present a model of amorphous silicon generated by a molecular dynamics (MD) simulation of a high-temperature anneal of an amorphous silicon sample using a quantum-mechanical (QM) model to compute forces. This procedure produces a new structure whose features are determined by QM energetics. The annealed model shows good agreement with experiment for a range of properties, and energetically stable deviations from four-fold coordination. In the annealing we have used a tight-binding method that the standard NRL-TB method, which does not include charge self-consistency. Analysis of the final structure shows that charge self-consistency changes the electronic structure significantly but has almost no effect on the geometry and total energies, even in the presence of coordination defects. All of these results are largely confirmed by *ab initio* density functional theory calculations.

In Sec. II we present some background information on experimental and simulation studies of the amorphous silicon structure, and we describe our simulation methods in Sec. III. We analyze the atomic structure, vibrational properties, and electronic structure of the relaxed and annealed samples using tight binding and density functional theory in Sec. IV. In Sec. V we discuss our results, and we give conclusions in Sec. VI.

II. BACKGROUND

Since *a*-Si is disordered, experimental atomic scale structural information is limited. Neutron and x-ray diffraction yield the radial distribution function,[4,5] including the effects of both static disorder inherent to the structure and dynamic disorder caused by zero-point and thermal motion. Some estimates of the bond angle distributions can also be extracted indirectly from the radial distribution function.[6] Additional information on bond lengths and numbers can be extracted from EXAFS,[7,8] and analyzing Raman peaks can give bond angle deviations.[9] Electron spin resonance, which is sensitive to unpaired electrons, gives indirect information about coordination defects,[10] and variable coherency transmission electron microscopy gives information about medium range order.[11,12] However, even basic questions about the structure, such as what deviations from fourfold coordination are present, are still unresolved.

Computer simulations have been widely used to study detailed structural information that cannot be obtained through experiment.[2,13–22] These simulations use special computational procedures to create and anneal an amorphous sample, either using a geometrically based algorithm,[2,13,21] fitting to experiment,[18] or by simulating a physical process such as quenching a liquid or low temperature deposition.[14–17,19,20]

 ©2006 The American Physical Society

However, the computational expense has limited these studies. Most of the simulations employed interatomic potentials, which are computationally efficient but do not capture the quantum-mechanical (QM) nature of the electrons that mediate interatomic bonding.[13–16,20,21] The few QM simulations were greatly limited in the amount of annealing, because the methods are computationally demanding.[17,19] One approach is to begin with a model that is annealed with an interatomic potential, and minimize its energy using QM computed forces.[23,24] However, in such a simulation with minimal or no annealing using QM forces it is unclear whether structural features such as coordination defects or the topology of the network actually reflect the QM energetics. Interpretation of comparisons with experimental results has been hindered by the size and time limitations in the computational work. Further, the effects of zero-point motion have only rarely been computed[24–27] or taken into account when comparing with experiment.[28]

III. METHODS

The structural model is generated by starting with a 216 atom continuous random network (CRN) model[29] created using a modified version of the Wooten-Winer-Weaire (WWW) geometrical algorithm that allows for four-membered rings.[13,30] This model is relaxed and annealed with forces computed using the Naval Research Lab (NRL)-TB total energy method[31–34] Si parametrization,[35] which uses a nonorthogonal sp^3 basis and environment dependent on-site energies. A model that we designate TB relaxed (TBR) is generated by relaxing the CRN cell and coordinates using the conjugate-gradient algorithm[36] with TB forces. This structure was discussed in two previous publications.[24,28] The sample is then annealed using a constant energy and constant volume MD simulation with the predictor-corrector algorithm[37] and a 1 fs time step. To stabilize the dynamics when atoms fluctuate close together to chemically irrelevant interatomic distances, we add a hardcore repulsion in the form of a pair potential contribution to the total energy. This potential has the form

$$V_{\mathrm{rep}} = \sum_{\langle ij \rangle} \begin{cases} \exp\left(\dfrac{r_O - r_I}{r_{ij} - r_I} + \dfrac{r_O - r_I}{r_{ij} - r_O}\right), & r_{ij} < r_O, \\ 0, & r_{ij} \geq r_O \end{cases} \qquad (1)$$

with $r_I = 1.85$ Å and $r_O = 2.05$ Å. The TBR is used as the starting point for the MD simulation, with random velocities consistent with a kinetic energy corresponding to $T = 1300$ K. The anneal is performed at constant energy for about 1.2 ns (1.2×10^6 time steps), and then quenched. The quenching process proceeds by a sequence of ~35 ps constant energy anneals, and the kinetic energy is reduced by about 10% between each annealing stage. This slow quench continues until the temperature is about 600 K, when diffusion and connectivity changes are negligible over the 35 ps time scale. The structure is again relaxed with the conjugate gradient algorithm and TB forces to produce the final annealed structure that we designate TB annealed (TBA).

The annealing process is intended to be carried out below the melting point of *a*-Si. From experiment, crystalline Si melts at 1675 K, and *a*-Si melts at 1420 K.[38] The precise melting points predicted by the TB model for the crystalline and amorphous phases are not known, although for the crystal it is estimated via the Lindemann criterion[39] to be around 1800 K.[35] We have verified that the pair correlation function during the anneal (not shown) has a distinct first neighbor peak and a minimum value of nearly zero between the first and second peaks, indicating that the structure during annealing is solidlike. The diffusivity (see Sec. IV A 1) is also much lower than the experimental liquid-phase value of 4×10^{-4} cm^2/s.[40]

Analysis of the electronic structure of the TBR and TBA structures is done using the charge-self-consistent (CSC) version of the NRL-TB method[41,42] with $U = 10$ eV, in order to enforce approximate local charge neutrality. To check our TB geometry and electronic structure results we also use first principles density-functional theory (DFT) calculations.[43,44] The initial CRN structure is relaxed using the Broyden-Fletcher-Goldfarb-Shanno method with DFT forces to produce a structure that we designate DFT relaxed (DFTR). The system at the end of the MD anneal and quench is relaxed to produce a structure that we designate TBA-DFTR. The TB and DFT relaxed atomic positions differ by less than 10% of the nearest neighbor (NN) distance between (neglecting the 0.4% difference in lattice constants), so discussions of atomic structure below focus on the TB relaxed structures. To summarize, we consider four structures, all starting from a CRN structure: the unannealed TBR and DFTR structures, and the annealed TBA and TBA-DFTR structures.

IV. RESULTS

A. Annealing

During the annealing process, the sample is simulated at constant energy with a temperature high enough to allow for significant atomic motion, including point-defect formation and annihilation, as well as diffusion. In principle, if this annealing is carried on long enough, the final structure will not carry any trace of the original geometry; it will simply be an equilibrium configuration consistent with the QM energetics that drive the annealing algorithm. To monitor this transformation we track the diffusion of the atoms and changes in the bonding. The diffusion is monitored by measuring the mean squared displacement of atoms relative to their initial positions. The slope of this quantity as a function of time is the self-diffusivity. One way we monitor changes in bonding is by periodically computing the neighbor list of each atom, and comparing it to the initial neighbor list. Another is by making a list of rings and comparing it to the initial list of rings. These two analyses give quantitative measures of the degree of commonality between the initial and annealed structures.

1. Diffusion

The mean squared displacement of each atom was calculated every 1000 time steps (1 ps) by subtracting the current position of the atom from its initial position, and averaging the squared magnitude of the distance over the configuration.

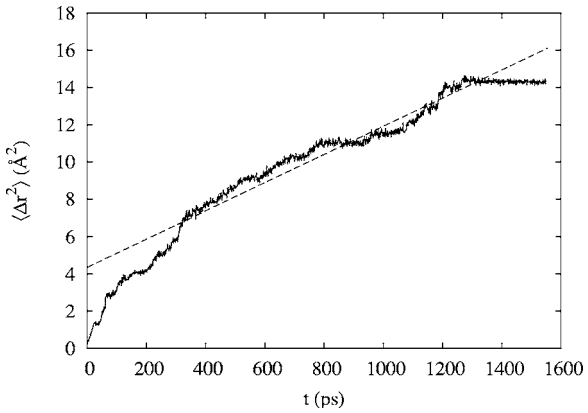

FIG. 1. Mean squared displacement of each atom as a function of time during annealing (solid line) and linear fit (dashed line).

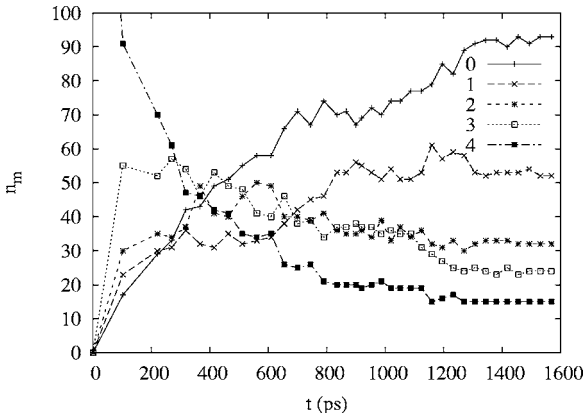

FIG. 2. Number of atoms n_m that have m neighbors in common with the initial (TBR) configuration as a function of annealing time.

This quantity is plotted in Fig. 1. During the annealing process atoms move an average of 3.74 Å, a small but significant distance on the atomic scale. This distance is comparable to the second neighbor distance in the crystal, so there could be significant rearrangement in the structure.

To compute a diffusivity we fit the mean squared displacements to a straight line over a time range from 200 to 1200 ps, which excludes an initial transient period and the quenching process. The slope from the fit is 7.6×10^{-7} cm^2/s. This number is much higher than our estimate of 1.6×10^{-12} cm^2/s from the experimental results in Ref. 45. It should be noted that the experimental estimate involves extrapolations both in temperature, from about 700–1300 K, and in composition, from an a-SiGe alloy to pure a-Si. Since the annealing temperature is probably close to the melting point, this extrapolation may be unreliable. Soon after the quenching process begins at $t=1.2$ ns the diffusion slows down greatly, and once the temperature goes to about 1100 K the diffusion becomes negligible over the simulation time scales.

2. Network connectivity

Since the goal of the simulation is to create an amorphous structure that is representative of the energetics of the QM description of bonding, it is important to determine how much of the original bonding in TBR remains in the final relaxed TBA structure. We monitor two quantities during the annealing process to determine the degree of similarity: the neighbor list of each atom, and the list of rings up to size eight. In Fig. 2 we plot the number of atoms n_m that have m unchanged neighbors. We define atoms as neighbors if they are within 2.8 Å (see also Sec. IV B 1). The number of atoms that have four of their neighbors unchanged (this corresponds to all of the neighbors for nondefect atoms) decreases rapidly, reaching about 15 (out of 216) by the end of the annealing. The number of atoms that have no neighbors in common with their initial configuration increases to about 90 during the anneal, and an additional 50 atoms have only one neighbor in common. This proves that the majority of the atoms have almost completely changed their local environment, and that the local structure in the TBA model should be mostly unrelated to the geometry of TBR.

The neighbor-list-change measure quantifies the change in local order, but there is also longer range order in the amorphous structure. We monitor changes on this intermediate length scale by computing the list of rings up to size 8 at different times during the annealing process. The number of initially existing rings that remain as a function of time is plotted in Fig. 3. The number of rings that remain intact quickly drops from the total number of rings in the TBR structure (950) to about 32 half way through the annealing, and then saturates. This drop indicates that the intermediate range structure that governs the topology of the network in the final TBA structure is almost completely unrelated to the initial TBR structure.

One question that remains is what are the specific bond rearrangement mechanisms that take place during annealing. For example, does the geometrical algorithm proposed by Wooten, Winer, and Weaire[13] correspond to the actual motion of the atoms? Such details are difficult to extract from the simulation. There are many atoms, many steps in the trajectory, and large amplitude thermal vibration that would need to be filtered out. However, the deviations from fourfold coordination observed during the annealing (15 at. %) and remaining after the slow quench (3.5 at. %) already indicate that the WWW mechanism, which always maintains fourfold coordination, is probably not sufficient to represent all

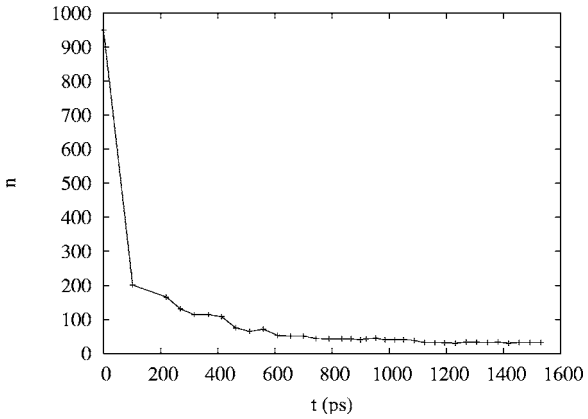

FIG. 3. Number of rings n up to size 8 in the initial (TBR) configuration that remain intact as a function of annealing time.

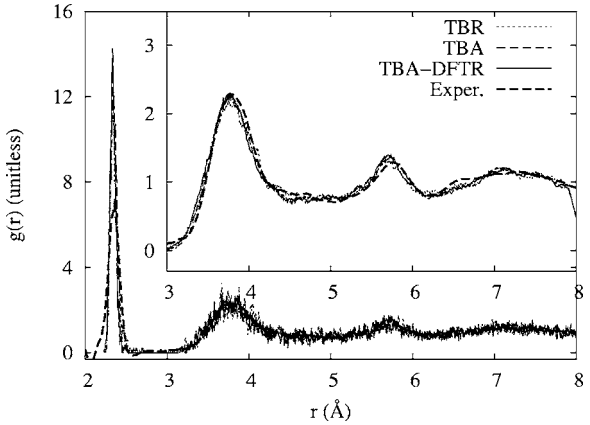

FIG. 4. Pair correlation function for TBR (dotted line), TBA (dashed line), and TBA-DFTR (thin solid line) models, as well as the experimental full peak (thick dashed line) from Ref. 5. The inset shows smoothed results for distance range beyond first neighbors with an expanded vertical scale.

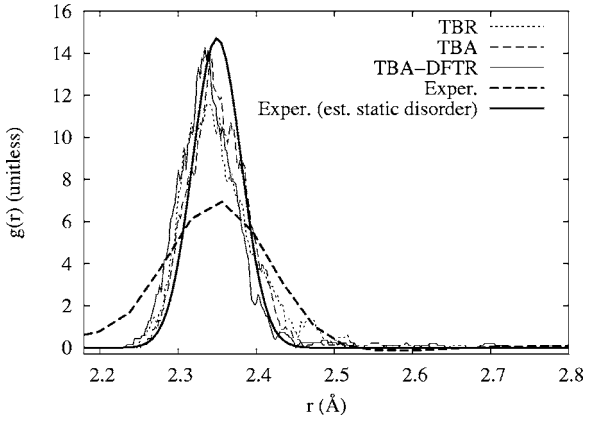

FIG. 5. First peak of the pair correlation function for TBR (dotted line), TBA (dashed line), and TBA-DFTR (thin solid line) models, as well as the experimental full peak (thick dashed line) and estimated static disorder contribution (thick solid line) from Ref. 5. The experimental static disorder estimate is plotted assuming the experimental coordination number of 3.88.

of the bond rearrangements that occur in MD. A detailed analysis, using the approach of Ref. 46, will be the subject of future research.

B. Structure

1. Pair correlation and angular distribution functions

The static pair correlation functions for the TBR and TBA models are shown in Fig. 4. The main plot shows pair correlation functions with a rectangular broadening width of 0.02 Å, and the inset shows the larger r range with a broadening width of 0.2 Å. There is very little change due to the annealing visible on this scale. The first neighbor peak is much sharper than the experimental result, as expected for a comparison of a static pair correlation function with a zero-point broadened experimental measurement.[24,28] The first neighbor peak is analyzed in more detail below. Beyond the first neighbor distance range, the agreement with experiment is very good even for the static RDF. As our previous analyses have shown,[24,28] zero-point motion leads to only subtle changes at these interatomic distances.

The first peak does undergo some change upon annealing, as Fig. 5 shows: annealing sharpens the peak, moves the maximum to larger distances, and makes the peak more symmetric by eliminating most of the tail at large interatomic distance. A similar result is seen in the DFTR and TBA-DFTR structures (the latter is also plotted in Fig. 4), although the peaks are slightly higher and narrower than the TB relaxed structures. The change in peak shape upon annealing is significant for interpreting experimental results.[24] The emergence of a symmetric peak shape only after annealing significantly modifies the results in Ref. 24 (which used a model equivalent to TBR), and again emphasizes the importance of annealing, not just relaxing, with a QM method in generating a representative amorphous structure. Our current results provide some theoretical validation of the Gaussian peak model used by Laaziri *et al.*[5] Direct comparison with experiment is difficult because of the challenges in obtaining high spatial resolution experimental diffraction data and because of the effects of zero-point and thermal motion. The analysis performed by Laaziri *et al.* from their x-ray diffraction measurements at $T=10$ K on both amorphous and crystalline silicon gives a static disorder parameter $\sigma=0.031$ Å.[5,47] The value of σ for the TBA-DFTR structure is sensitive to the precise cutoff distance used. If we include only the main peak ($r<2.45$ Å), we find $\sigma=0.035$ Å, in good agreement with experiment. A less ambiguous comparison can be made by examining the height of the first neighbor peak of $g(r)$ (Fig. 5). For the TBA-DFTR structure we get a peak height of 14.0, as compared with 14.7 for the estimated static disorder peak by Laaziri *et al.* For comparison, the raw experimental peak (measured at $T=10$ K, or about 2% of the Debye temperature), which includes both static disorder and zero-point motion, has a much smaller height of about 7.

Earlier TB MD work by Servalli and Colombo[19] reported pair correlation function results from a simulation of the quench of a liquid. The resulting structure had an overly broad first neighbor peak, with a height of about 7 as compared with about 15 from experiment, as we discuss above. This difference may be a result of the short quench and brief, low temperature anneal mandated by the computational expense of the simulation. One of the best CRN models, constructed by Barkema and Mousseau,[2] using a procedure based on the WWW algorithm,[13] showed perfect fourfold coordination, a narrow bond angle distribution, and very low energy as evaluated by interatomic potentials. However, its pair correlation function first neighbor peak is also too broad. In fact, the static peak height is even lower than the raw experimental peak (as seen in Fig. 4 of Ref. 2).

The minimum between the first and second neighbor peaks is around 2.8 Å, so we use that distance to define "nearest neighbors" geometrically. The physical significance of this criterion is discussed further is Sec. IV E. The bond angle distribution function is plotted in Fig. 6. In this plot we see minor differences that arise during the annealing process. The main peak, centered just above the ideal tetrahedral

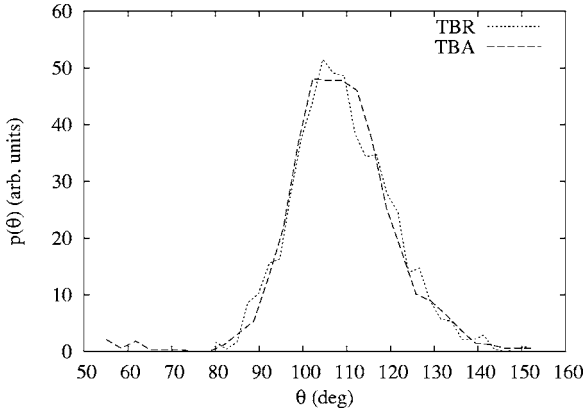

FIG. 6. Bond angle distribution function for TBR (solid line) and TBA (dashed line) models.

angle of 109.5°, is significantly smoother after annealing, although its peak position, peak value, and width are essentially unchanged. A more interesting change is that a small peak has developed near 60°, associated with coordination defects (see Sec. IV B 2). The presence of small angles are consistent with the findings of Kugler *et al.*,[48] and may explain the presence of electronic states in the gap (Sec. IV E). Quantitative measures of the pair correlation and angular distribution function peaks are listed in Table I. Experimental estimates from diffraction experiments give bond-angle peak widths of 11°.[4] Unfortunately, quantitative results from earlier TB MD work[19] is not available. We do find a significantly narrower range of bond lengths, and a slightly broader range of bond angles, as compared with the latest CRN models.[2] These differences are consistent with our sharper and taller pair correlation function first neighbor peak, which is in better agreement with experimental results than the CRN models.

2. Coordination number statistics

One important question about amorphous silicon is whether it is perfectly fourfold coordinated in equilibrium. It is clearly possible to create reasonably low energy fourfold coordinated amorphous structures, e.g., using the WWW method, but it is not clear that these are necessarily the lowest energy structures. Since this question involves the existence of dangling and floating bonds,[49] a quantum-mechanical description of bonding is expected to be important. In Table I we list the concentration of atoms of each coordination present in the sample, from 3 to 6. The coordination is defined using the same geometrical criterion for nearest neighbors as used elsewhere in this work. The TBR structure is perfectly fourfold coordinated, as in the CRN model from which it is derived. The TBA structure, on the other hand, shows a number of coordination defects. Overcoordinated atoms dominate, although some undercoordinated atoms are also present. The precise numbers depend on whether weak bonds (see Sec. IV E) are included. Both over and undercoordinated defects have been extensively investigated in the past. It has been argued that both dangling[50–53] and floating[49,54–56] bonds are needed to explain experimental data.[10,57,58] The presence of overcoordinated atoms in structural models is often ascribed to the fast quenching from the liquid phase (which is six-fold coordinated). Our method does not involve a liquid structure and overcoordinated defects are spontaneously formed during annealing of the CRN structure. Earlier TB MD work that simulated quenching of an overcoordinated liquid also showed roughly equal numbers of undercoordinated and overcoordinated atoms,[19] although at higher concentrations. The differences may be caused by the large differences in annealing times and temperatures, or by the choice of TB models. Directly comparing these results to experiment is not possible because experimental probes can not detect coordination defects. Indirect measurements based on electron spin resonance and carrier lifetime exist, but it is not possible to relate them quantitatively to coordination defect densities.

The positions of the defect atoms are visualized in Fig. 7. There is distinct clustering of the overcoordinated atoms, but none apparent for the undercoordinated atoms. The coordination defects appear to be an equilibrium property of the TB description of amorphous silicon, since they also correspond to a lower formation energy (Table I). The energy gain could be attributable to the presence of the defects themselves, or to the changes in the bond length distributions reflected in

TABLE I. Structural properties: mean nearest neighbor distance r_{NN}, root mean squared (r.m.s) neighbor distance deviation Δr_{NN}, bond angle distribution main peak mean θ_0 and width (r.m.s) $\Delta\theta_0$, concentration of atoms n_m with coordination m, number of minimal rings per atom r_l of size l, number density ρ, energy per atom relative to the crystal without E and with E^{CSC} charge self-consistency, and elastic constants c_{ij}. Crystal elastic constants are from Ref. 35.

	crystal	TBR	TBA
r_{NN} (Å)	2.35	2.36	2.36
Δr_{NN} (Å)	0.0	0.048	0.044
θ_0 (deg.)	109.5	109.2	109.1
$\Delta\theta_0$ (deg.)	0.0	11	11
n_3	0	0	0.93%
n_4	100%	100%	97%
n_5	0	0	1.9%
n_6	0	0	0.46%
r_3	0	0	0.028
r_4	0	0.028	0.014
r_5	0	0.44	0.51
r_6	2	0.75	0.62
r_7	0	0.52	0.48
r_8	0	0.17	0.15
r_9	0	0.042	0.074
r_{10}	0	0.0046	0.0046
ρ (Å^{-3})	0.0501	0.0494	0.0497
E (eV)	0.0	0.217	0.189
E^{CSC} (eV)	0.0	0.220	0.194
c_{11} (GPa)	179	165±1.3	163±0.4
c_{12} (GPa)	73	49.2±0.9	48.6±0.6
c_{44} (GPa)	95	57.8±0.5	57.1±0.2

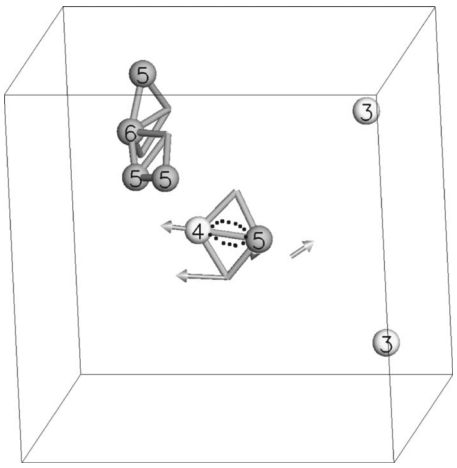

FIG. 7. Visualization of coordination defects, labeled by geometric coordination (most four-fold coordinated atoms are not shown), bonds corresponding to three-membered rings, and quasilocalized eigenvector displacement amplitudes (arrows). The highlighted bond is weak (Sec. IV E), and therefore the coordination of adjacent atoms may be lower by one and the adjacent three-membered rings may be unphysical.

the first peak of the pair correlation function. It is impossible to separate these effects, and in fact it may be that the existence of the defects is needed to produce the sharp, symmetric peak observed by us and in experiment.[5] If the energy difference is attributed entirely to the coordination defects, it corresponds to an average energy gain of 0.9 eV per defect atom. Our DFT total energy results confirm the TB results. The DFT energy for the amorphous models relative to the crystal is about 0.17 eV per atom, close to the TB value of about 0.20 eV/atom. More importantly, the energy difference between the DFTR and TBA-DFTR is of the same order as the corresponding TB energy difference, showing an energy gain of about 0.5 eV per defect atom.

3. Ring statistics

While coordination number statistics give information about short range order, ring statistics reveal medium range order. We have computed the number of minimal rings[59] (rings that cannot be decomposed into two smaller rings) up to size 10. The results are listed in Table I. For reference, the crystal has two six-membered rings per atom. In the TBR structure there is a predominance of six-membered rings, with substantial numbers of five- and seven-membered rings as well. There are also a few four-membered rings, and some larger rings including one ten-membered ring. Annealing the structure with TB reduces the overall number of rings, in particular six-, seven-, and eight-membered rings, although the number of five-membered rings increases. A small number of three-membered rings are formed, and there is one ten-membered ring, although it consists of different atoms than the ten-membered ring in the TBR structure. If we treat weak bonds (see Sec. IV E) as broken bonds, these numbers change slightly: two of the three-membered rings are eliminated (r_3=0.019) and one four-membered ring is created (r_4=0.019). The well relaxed CRN model by Barkema and Mousseau[2] had very similar ring statistics overall, although they did not observe any ten-membered rings, and only some versions of the model had four-membered rings. This similarity suggests that a wide range of short range structural features (e.g., coordination defect concentrations and bond length distributions) can be present in structures with very similar medium range order.

A visualization of the three-membered rings in Fig. 7 shows that they are not randomly distributed. The rings themselves occur in edge-sharing pairs, and all are associated with overcoordination defects. This is presumably not the case for the four-membered rings, since those exist even in the TBR structure which is perfectly four-fold coordinated.

C. Density and elastic constants

To assess whether the microscopic structural changes lead to changes that can be observed macroscopically, we analyzed the simulation cell density and elastic properties of the TBR and TBA models. The densities are listed in Table I. The annealing process produces a density change of only +0.6%, despite the significant changes in bonding topology and point defect concentration. The TBA density is about 0.8% lower than the crystal, as compared with a difference of 1.7% measured experimentally.[6]

The elastic constant matrix gives mechanical property information about the material. The constants were computed from finite-difference derivatives of the stress with respect to strain. We applied 0.1 and 0.2 % strains to the TBR and TBA models, relaxed the atomic positions, and evaluated the stress in the deformed cell. The stress values at the two different strains were compared in order to confirm that the deformation was in the linear regime. In Table I we list the elastic constant matrix elements, averaged over different orientations assuming that the system has maximal (cubic) symmetry. In fact, our elastic constants are quite isotropic, and satisfy the relation

$$c_{44} = \frac{(c_{11} - c_{12})}{2} \tag{2}$$

quite well. The error estimates in the table reflect the root mean squared deviation between the different matrix elements that contribute to each average value. The TBR elastic constants are in very good agreement with our previous calculations,[24] and do not show significant change in magnitude after the annealing process. This indicates that despite the changes in bonding and point defect concentration, there is no evidence of aging in the infinitesimal-deformation mechanical properties. The error estimates, which quantify the anisotropy in the sample caused by the finite size of the simulation, are about twice as small after annealing, indicating that the TBA structure is substantially more isotropic than the TBR structure.

D. Vibrational density of states

Another view of the type and strength of bonding and disorder in the structure comes from the vibrational density of states (VDOS). We compute the full force-constant matrix

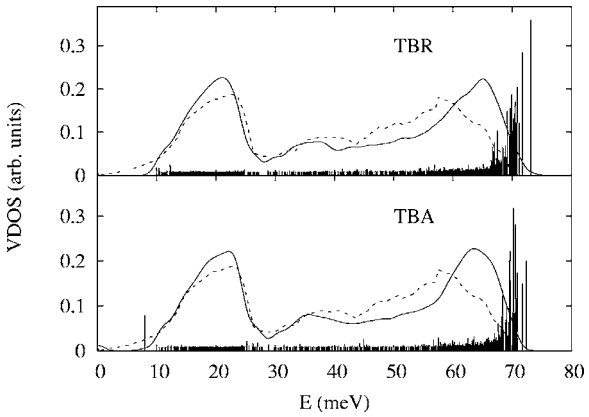

FIG. 8. VDOS for simulated structure (solid line), VDOS for experiment (Ref. 66) (dashed line), and IPR (solid impulses).

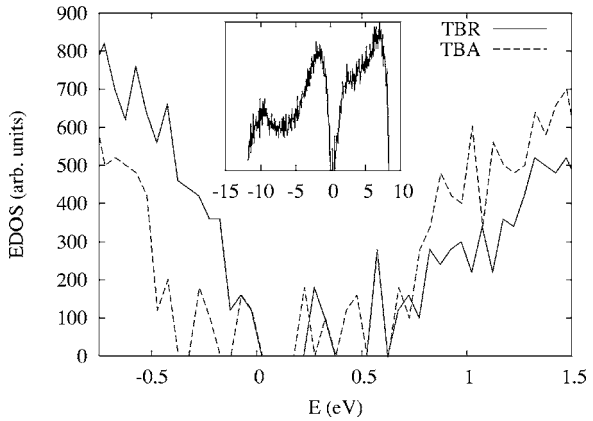

FIG. 9. Electronic density of states for the TBR (solid line) and TBA (dashed line) structures near the Fermi level ($E=0$) computed using the CSC NRL-TB method. Inset: complete EDOS for the TBR structure, which is nearly identical, except in the gap region, to the TBA EDOS.

by calculating the forces for displaced atom positions. We take positive and negative displacements to remove odd order anharmonic terms in the potential, and two values of displacement in order to check that even order anharmonic terms are not significant. From the eigenvalues of the force constant matrix we calculate the VDOS and from the eigenvectors the inverse participation ratio (IPR).[60] As can be seen from Fig. 8 the VDOS is qualitatively, if not quantitatively, quite accurate. This is true for both the TBR (previously published in Ref. 24) and TBA structures. The main difference between the results for TBA and TBR seems to be the single low frequency possible quasi-localized mode, indicated by the IPR peak below 100 meV. Such modes have been observed in calculations based on empirical potentials for several glassy and amorphous systems including amorphous silicon.[24,61–63] They may also have experimental significance for the boson peak that is observed in glassy systems, although apparently not in amorphous silicon to our knowledge.[64] On the other hand, they could also be due to finite size effects.[65] The displacement eigenvector of the quasilocalized mode is visualized in Fig. 7 and it is clear that it is associated with a *structural* defect. It seems to be concentrated around an atom with four-fold geometric coordination but with only three strong bonds to its neighbors.

E. Electronic structure

Defects in the bonding topology are often associated with electronic states in the band gap of silicon. To determine the effects of the TBR and TBA geometries on electronic structure we calculated electronic density of states (EDOS) by computing a histogram of the electronic eigenvalues. Since conventional TB calculations, without charge self-consistency, can lead to spurious charge transfer, especially near defects, we compared our TB results to calculations using a charge-self-consistent (CSC) version of the TB model.[41,42] We used the CSC TB method to evaluate the total energy and electronic structure for the TBR and TBA structures, and found only small changes to the total energies of the two structures (Table I). The energies relative to the crystal increase by about 1–3 %, and the difference between the two decreases from 0.028 to 0.026 eV/atom. Relaxing both structures produces minimal structural changes, with atoms moving less than 0.1 Å.

The EDOS, on the other hand, shows significant effects due to the charge rearrangement. In the non-self-consistent TB results (not shown), both structures have gaps of about 0.6 eV, and the TBA structure has no gap states despite the presence of coordination defects, a result that seems unphysical. The CSC-TB results, plotted in Fig. 9, show that both structures have gaps containing a few electronic states. We define the gap states as those that appear to be separated from the continuous bands. In the TBR structure the gap between occupied and unoccupied bands is about 0.6 eV, and there are two unoccupied states in the gap. The annealing process, which creates coordination defects in the TBA structure, leads to a wider gap of about 1 eV, but with more gap states. Two of these gap states are occupied, and three more are unoccupied. The gap size and positions of gap states are confirmed by the DFT calculations on the TBA-DFTR structure. Gap states in CRN models have previously been observed,[67] and may be associated with the presence of small bond angles, as discussed by Kugler *et al.*[48]

By analyzing the electronic structure, we can determine if the overcoordination is apparent in the interatomic bonding, or if it is simply a geometric construct with no underlying physics. Using our CSC TB method, we compute overlap occupations[68,69] between atoms I and J

$$n_{IJ} = \sum_{i \in b(I), j \in b(J)} S_{ij}\rho_{ij}, \tag{3}$$

where S is the overlap matrix, ρ is the occupied state density matrix, and $b(I)$ is the set of basis orbitals associated with atom I. A sum over J of n_{IJ} gives the Mulliken population on atom I.[68,69] In the DFT calculations, which use a plane wave basis, we project the wave function on atomic orbitals to analyze electron localization.

In the TBR model, where all atoms are geometrically fourfold coordinated, the overlap occupations for geometric nearest neighbors range from 0.07 to 0.11 (in arbitrary units).

The largest overlap occupation for a pair of atoms that lie beyond the maximum NN distance (2.8 Å) is only 0.002. In the TBA model we examined the overlap occupation for each atom, and compared the geometric coordination with the number of relatively strong bonds. The geometrically undercoordinated atoms each have three roughly equally strong bonds (0.082–0.097), and much weaker bonds to other atoms ($\leq$0.013). The one sixfold coordinated atom has six significant bonds of varying strength, with overlap occupation ranging from 0.032 to 0.095. All but one of the fivefold coordinated atoms have two or three strong bonds (0.087–0.105), with the remainder of the bonds somewhat weaker (0.042–0.062). There is one very weak bond (0.015, highlighted in Fig. 7) between atoms within the geometrical cutoff: a four-fold coordinated atom and a five-fold coordinated atom at a distance of 2.7 Å. It may be more accurate to regard these two atoms as three-fold and four-fold coordinated, respectively. This interpretation would decrease the number of five-fold coordinated atoms by one, yielding $n_5 = 1.4\%$, and increase the number of three-fold coordinated atoms by one, yielding $n_3 = 1.4\%$.

V. DISCUSSION

The definition of coordination in atomistic models of *a*-Si is usually based on geometry, i.e., a critical distance below which two atoms are considered to be neighbors. While this approach is natural in an interatomic potential simulation, quantum-mechanical methods allow for definitions based on the presence or absence of electrons in the covalent bond. Our comparison of the two definitions shows that the geometric criterion for defining neighbors, and therefore coordination $r \leq 2.8$ Å is consistent with the electronic structure in all but one case; there is one very weak apparent bond, with $r = 2.7$ Å. However, a geometric criterion with a shorter cutoff of about 2.65 Å is fully consistent with the electronic structure analysis of bonding. We also note that the overcoordinated atoms are clustered, and associated with three-membered rings. The undercoordinated atoms are dispersed, and one is associated with a very soft quasilocalized vibrational mode with a high IPR.

The first peak of the pair correlation function shows subtle changes between the TBR and TBA structures. The peak in the latter structure is sharper and more symmetric, but not precisely Gaussian in shape. The symmetric peak shape is consistent with analysis of experimental data by Laaziri *et al.*, and stands in contradiction with our earlier work on the TBR structure.[24] The height of the peak is in much better agreement with the extracted static disorder $g(r)$ of Laaziri *et al.* [computed by us using their Gaussian $J(r)$] than earlier TB MD results and very well relaxed CRN structures.

The presence of coordination defects in the TBA structure is associated with a lower energy and larger band gap than the perfectly four-fold coordinated TBR structure. It is not possible to determine whether this energy gain is associated with the defects themselves or with the changes in the bond length reflected in the pair correlation function. Even if they are not directly energetically favored, the coordination defects may very well be necessary for obtaining the sharp first neighbor peak that can lead to a lower energy overall. The energy comparison is clearly dependent on the choice of reference CRN structures. While our initial structure is not the most relaxed CRN structure available, we note that we find a total energy for the TBA structure that is marginally lower than the TB-relaxed version of a very well relaxed Barkema and Mousseau 1000 atom structure.[28] However, this comparison is not exact because of differences in system size and unit cell shape constraints. The TBR structure has a finite band gap, as expected for a perfectly fourfold coordinated Si structure, although there are unoccupied states in the gap, presumably associated with defect levels. The TBA structure, with its coordination defects, has a wider gap than the TBR structure, but some of the defect states in the gap are occupied.

Our first principles DFT calculations validate the TB results. Structural changes induced by DFT relaxation are minimal, and the topology of the network is unchanged. The DFT results confirm the observation of energetically favorable coordination defects and the features in the pair correlation function and EDOS.

We have calculated four experimentally observable quantities: pair correlation function, elastic constants, VDOS, and EDOS. None of these measures show large changes between the TBR and TBA structures, despite the changes in bonding topology and coordination defect concentrations. The first peak of the pair correlation function of the TBA structure is somewhat sharper and more symmetric, and this structure has a low frequency quasilocalized vibrational mode which could manifest itself in neutron scattering or specific heat measurements. However, the small size of the sample makes it difficult to determine whether this vibrational mode represents a real, although low concentration, feature of bonding.

VI. CONCLUSIONS

We have generated an amorphous silicon structure using tight-binding molecular dynamics annealing at 1300 K for over 1.2 ns. Tracking short and medium range order during the annealing process indicates that bonding topology in the final structure is largely uncorrelated with the initial continuous random network structure. We find significant microscopic changes, including the formation of 3.5% coordination defects and changes in ring statistics. Annealing also produces a sharper and more symmetric first neighbor peak in the pair correlation function, bringing it into good agreement with experiment. The total energy (relative to the crystal) for the annealed structure with the coordination defects is about 10% lower than that of the initial amorphous structure. These results show that the perfectly fourfold coordinated CRN structure is not necessarily the lowest energy structure. Structures with coordination defects, including overcoordinated atoms, can be energetically stable rather than existing only as artifacts of an overcoordinated liquid initial state. The annealed structure is slightly less dense than the crystal and has a significant band gap with occupied and unoccupied defect levels. The only signature of the coordination defects is a very low frequency quasilocalized vibrational mode associated with one defect.

We have shown that it is possible to anneal a good CRN structure and produce a structure with coordination defects that is in better agreement with the experimental pair correlation function and lower in energy. Additional work could be useful in further improving the annealed structure. Different initial structures and longer simulations could eliminate the remaining traces of the initial geometry. Improved approximations, for example, charge-self-consistency terms used during annealing and constant pressure (rather than constant volume) molecular dynamics, could also improve the reliability of the annealing procedure. Finally, more detailed analyses of the effects of zero-point motion and of the detailed atomic bond rearrangement mechanisms that occur during annealing will enable more precise comparison to experiment and shed light on the microscopic annealing processes.

ACKNOWLEDGMENTS

N.B. and J.L.F. acknowledge the support of ONR and NRL, and the support of the DOD HPCMPO CHSSI program in developing the TBMD software.[70] We thank D. A. Papaconstantopoulos and M. J. Mehl for helpful suggestions. The first principles calculations were performed using the QUANTUM-ESPRESSO package[43] with the support of the Research Excellence Fund of the State of Michigan. We are also grateful to S. Roorda for sending us the x-ray data of Ref. 5.

[1] B. Kramer and D. Weaire, in *Amorphous Semiconductors*, edited by M. Brodsky (Springer, Berlin, 1979), Vol. 36.
[2] G. T. Barkema and N. Mousseau, Phys. Rev. B **62**, 4985 (2000).
[3] L. Pusztai and S. Kugler, J. Phys.: Condens. Matter **17**, 2617 (2005).
[4] J. Fortner and J. S. Lannin, Phys. Rev. B **39**, R5527 (1989).
[5] K. Laaziri, S. Kycia, S. Roorda, M. Chicoine, J. L. Robertson, J. Wang, and S. C. Moss, Phys. Rev. Lett. **82**, 3460 (1999), and references therein; Phys. Rev. B **60**, 13 520 (1999).
[6] J. S. Custer, M. O. Thompson, D. C. Jacobson, J. M. Poate, S. Roorda, W. C. Sinke, and F. Spaepen, Appl. Phys. Lett. **64**, 437 (1994).
[7] M. Wakagi, K. Ogata, and A. Nakano, Phys. Rev. B **50**, 10666 (1994).
[8] A. Filipponi, F. Evangelisti, M. Benfatto, S. Mobilio, and C. R. Natoli, Phys. Rev. B **40**, 9636 (1989).
[9] D. Beeman, R. Tsu, and M. F. Thorpe, Phys. Rev. B **32**, 874 (1985).
[10] J. H. Stathis, Phys. Rev. B **40**, 1232 (1989).
[11] J. M. Gibson and M. M. J. Treacy, Phys. Rev. Lett. **78**, 1074 (1997).
[12] M. M. J. Treacy, J. M. Gibson, and P. J. Keblinski, J. Non-Cryst. Solids **231**, 99 (1998).
[13] F. Wooten, K. Winer, and D. Weaire, Phys. Rev. Lett. **54**, 1392 (1985).
[14] M. D. Kluge, J. R. Ray, and A. Rahman, Phys. Rev. B **36**, 4234 (1987).
[15] P. C. Kelires and J. Tersoff, Phys. Rev. Lett. **61**, 562 (1988).
[16] W. D. Luedtke and U. Landman, Phys. Rev. B **37**, 4656 (1988).
[17] I. Stich, R. Car, and M. Parrinello, Phys. Rev. B **44**, 11092 (1991).
[18] S. Kugler, L. Pusztai, L. Rosta, P. Chieux, and R. Bellissent, Phys. Rev. B **48**, 7685 (1993).
[19] G. Servalli and L. Colombo, Europhys. Lett. **22**, 107 (1993).
[20] G. H. Gilmer and C. Roland, Appl. Phys. Lett. **65**, 824 (1994).
[21] G. T. Barkema and N. Mousseau, Phys. Rev. Lett. **77**, 4358 (1996).
[22] S. M. Nakhmanson, P. M. Voyles, N. Mousseau, G. T. Barkema, and D. A. Drabold, Phys. Rev. B **63**, 235207 (2001).
[23] S. M. Nakhmanson and D. A. Drabold, Phys. Rev. B **58**, 15325 (1998).
[24] J. L. Feldman, N. Bernstein, D. A. Papaconstantopoulos, and M. J. Mehl, Phys. Rev. B **70**, 165201 (2004).
[25] C. P. Herrero, Europhys. Lett. **44**, 734 (1998).
[26] C. P. Herrero, J. Non-Cryst. Solids **271**, 18 (2000).
[27] C. P. Herrero, J. Phys.: Condens. Matter **12**, 265 (2000).
[28] J. L. Feldman, N. Bernstein, D. A. Papaconstantopoulos, and M. J. Mehl, J. Phys.: Condens. Matter **16**, S5165 (2004).
[29] F. Wooten (private communication).
[30] J. L. Feldman, J. Q. Broughton, and F. Wooten, Phys. Rev. B **43**, 2152 (1991).
[31] R. E. Cohen, M. J. Mehl, and D. A. Papaconstantopoulos, Phys. Rev. B **50**, 14694 (1994).
[32] M. J. Mehl and D. A. Papaconstantopoulos, Phys. Rev. B **54**, 4519 (1996).
[33] M. J. Mehl and D. A. Papaconstantopoulos, in *Topics in Computational Materials Science*, edited by C. Y. Fong (World Scientific, Singapore, 1998), Chap. 5, pp. 169–213.
[34] http://cst-www.nrl.navy.mil/bind/
[35] N. Bernstein, M. J. Mehl, D. A. Papaconstantopoulos, N. I. Papanicolaou, M. Z. Bazant, and E. Kaxiras, Phys. Rev. B **62**, 4477 (2000); **65**, 249902(E) (2002).
[36] W. H. Press, B. P. Flannery, S. A. Teukolsky, and W. T. Vetterling, *Numerical Recipes in FORTRAN*, 2nd ed. (Cambridge University Press, Cambridge, 1992).
[37] M. P. Allen and D. J. Tildesley, *Computer Simulations of Liquids* (Oxford University Press, Oxford, 1987).
[38] E. P. Donovan, F. Spaepen, D. Turnbull, J. M. Poate, and D. C. Jacobson, J. Appl. Phys. **57**, 1795 (1985).
[39] F. A. Lindemann, Phys. Z. **11**, 609 (1910).
[40] P. G. Sanders and M. J. Aziz, J. Appl. Phys. **86**, 4258 (1999).
[41] M. Elstner, D. Porezag, G. Jungnickel, J. Elsner, M. Haugk, T. Frauenheim, S. Suhai, and G. Seifert, Phys. Rev. B **58**, 7260 (1998).
[42] N. Bernstein, M. J. Mehl, and D. A. Papaconstantopoulos, Phys. Rev. B **66**, 075212 (2002).
[43] S. Baroni *et al.*, http://www.pwscf.org.
[44] For all the first principles calculations we used a norm-conserving pseudopotential generated with the recipe of Von-Barth and Car with plane-wave cutoff of 16 Ry. Forces and energies are well converged. Only Γ point had been used to integrate in reciprocal space.

[45] G. Q. Lu, E. Nygren, and M. J. Aziz, J. Appl. Phys. **70**, 5323 (1991).
[46] N. Bernstein, M. J. Aziz, and E. Kaxiras, Phys. Rev. B **61**, 6696 (2000).
[47] The broadening of the *a*-Si static disorder peak by zero-point motion has been confirmed theoretically (Refs. 24–28).
[48] S. Kugler, K. Kohary, K. Kádas, and L. Pusztai, Solid State Commun. **127**, 305 (2003).
[49] S. T. Pantelides, Phys. Rev. Lett. **57**, 2979 (1986).
[50] P. A. Fedders and A. E. Carlsson, Phys. Rev. B **39**, 1134 (1989).
[51] R. Biswas, C. Z. Wang, C. T. Chan, K. M. Ho, and C. M. Soukoulis, Phys. Rev. Lett. **63**, 1491 (1989).
[52] P. A. Fedders, D. A. Drabold, and S. Klemm, Phys. Rev. B **45**, 4048 (1992).
[53] J. M. Holender and G. J. Morgan, J. Phys.: Condens. Matter **4**, 4473 (1992).
[54] S. T. Pantelides, Phys. Rev. Lett. **58**, 1344 (1987).
[55] P. C. Kelires and J. Tersoff, Phys. Rev. Lett. **61**, 562 (1988).
[56] M. Fornari, M. Peressi, S. De Gironcoli, and A. Baldereschi, Europhys. Lett. **47**, 481 (1999).
[57] M. Kumeda and T. Shimizu, Jpn. J. Appl. Phys. **19**, L197 (1980).
[58] D. K. Biegelsen and M. Stutzmann, Phys. Rev. B **33**, 3006 (1986).
[59] S. V. King, Nature (London) **213**, 1112 (1967).
[60] R. J. Bell and P. Dean, Discuss. Faraday Soc. **50**, 55 (1970).
[61] V. L. Gurevich, D. A. Parshin, and H. R. Schober, Phys. Rev. B **67**, 094203 (2003), and references therein.
[62] J. Fabian, cond-mat/0104464 (unpublished), and references therein.
[63] R. Biswas, A. M. Bouchard, W. A. Kamitakahara, G. S. Grest, and C. M. Soukoulis, Phys. Rev. Lett. **60**, 2280 (1988).
[64] Two recent suggestions for the boson peak in amorphous silicon come from a study of voids and extreme disorder, respectively in S. M. Nakhmanson and D. A. Drabold, Phys. Rev. B **61**, 5376 (2000), and F. Finkemeier and W. von Niessen, *ibid.* **63**, 235204 (2001).
[65] J. L. Feldman, P. B. Allen, and S. R. Bickham, Phys. Rev. B **59**, 3551 (1999).
[66] W. A. Kamitakahara, C. M. Soukoulis, H. R. Shanks, U. Buchenau, and G. S. Grest, Phys. Rev. B **36**, 6539 (1987).
[67] J. J. Dong and D. A. Drabold, Phys. Rev. Lett. **80**, 1928 (1998).
[68] R. S. Mulliken, J. Chem. Phys. **23**, 1833 (1955).
[69] R. S. Mulliken, J. Chem. Phys. **23**, 1841 (1955).
[70] http://cst-www.nrl.navy.mil/bind/dodtb/